QCD thermodynamics with an improved lattice action

Claude Bernard and James E. Hetrick
Department of Physics, Washington University, St. Louis, Missouri 63130

Thomas DeGrand and Matthew Wingate
Department of Physics, University of Colorado, Boulder, Colorado 80309

Carleton DeTar
Department of Physics, University of Utah, Salt Lake City, Utah 84112

Steven Gottlieb
Department of Physics, Indiana University, Bloomington, Indiana 47405

Urs M. Heller
SCRI, Florida State University, Tallahassee, Florida 32306-4052

Kari Rummukainen
Fakultät für Physik, Universität Bielefeld, D-33615, Bielefeld, Germany

Doug Toussaint
Department of Physics, University of Arizona, Tucson, Arizona 85721

Robert L. Sugar
Department of Physics, University of California, Santa Barbara, California 93106

(MILC Collaboration)

(Received 7 March 1997; revised manuscript received 29 May 1997)

We have investigated QCD with two flavors of degenerate fermions using the Symanzik-improvement program for both the gauge and fermion actions. Our study focuses on the deconfinement transition on an $N_t=4$ lattice. Having located the thermal transition, we performed zero temperature simulations nearby in order to compute hadronic masses and the static quark potential. We find that this action reduces lattice artifacts present in thermodynamics with the standard Wilson (gauge and fermion) actions. However, comparisons between improved Wilson and Kogut-Susskind actions show some disagreement. [S0556-2821(97)02521-6]

PACS number(s): 12.38.Gc, 11.10.Wx, 12.38.Mh

I. INTRODUCTION

An understanding of the high temperature behavior of QCD is desirable in addressing problems such as heavy ion collisions and the evolution of the early universe. It is believed that, at a temperature between 140 and 200 MeV (where pions are produced copiously), hadronic matter undergoes a transition to a plasma of quarks and gluons. This phenomenon is intrinsically nonperturbative, and Monte Carlo lattice simulation provides the best theoretical tool with which to study it.

Most lattice studies have used Kogut-Susskind (KS) fermions because of their exact U(1) chiral symmetry at finite lattice spacing. The full SU(2) chiral symmetry is recovered in the continuum limit. Although in contrast Wilson fermions explicitly break chiral symmetry, the continuum limit of the different discretizations is expected to be the same. One advantage of simulating with two flavors of Wilson quarks versus two flavors of KS fermions is that the updating algorithm is exact in the former case but has finite time step errors in the latter. The price to be paid is that the explicit chiral symmetry breaking gives rise to an additive mass renormalization; thus, the location of the chiral limit is not known *a priori*.

Even more troublesome for dynamical Wilson fermions is the presence of lattice artifacts which qualitatively affect physics at large lattice spacing. In Refs. [1] and [2] it was found that the deconfinement transition becomes very steep for intermediate values of the hopping parameter κ. In fact, on an $N_t=6$ lattice the transition appears to be first order for a range of intermediate hopping parameters and smooth otherwise.

The lattice community has worked very hard recently to construct actions which have fewer lattice artifacts than the standard discretizations of the continuum action. One philosophy is to add operators to the action which cancel $O(a^n)$ terms in the Taylor expansion of spectral observables. It is plausible that an action which converges to the continuum action faster in the $a\rightarrow 0$ limit would be free of the artificial first order behavior. We adopt this improvement program, attributed to Symanzik, in the present work.

An alternative approach is to search for an action which

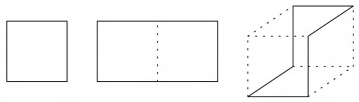

FIG. 1. The three Wilson loops in the one-loop Symanzik-improved gauge action that we used.

lies on or near the renormalized trajectory of some renormalization group transformation. Since all irrelevant couplings are zero along the renormalized trajectory, actions there have no scaling violations, i.e., are quantum perfect. Such an action was approximated by Iwasaki [3] and has been used to study QCD thermodynamics with two flavors of unimproved Wilson fermions [4]. Although it is still an open question to what extent this action lies on a renormalized trajectory, the results of Ref. [4] show improvement over standard Wilson thermodynamics.

In this paper we report on our simulation of finite temperature lattice QCD with two flavors of $O(a)$ Symanzik-improved fermions and $O(a^2)$ Symanzik-improved glue. We describe the action we used in Sec. II. In Sec. III we give the details of our simulations, and we present our results in Sec. IV. Finally, we give our conclusions in Sec. V.

II. ACTION

When one expands a lattice operator in a Taylor series about zero lattice spacing a, one recovers its relevant (or marginal) continuum operator plus higher dimensional irrelevant operators proportional to powers of a. Symanzik suggested that by selecting a favorable combination of lattice operators in the lattice action, one might have cancellations of the irrelevant operators up to some order in the lattice spacing [5]. Lüscher and Weisz have applied this philosophy to SU(N) gauge theories. They imposed an on-shell improvement condition whereby discretization errors are eliminated order by order in a from physical observables and constructed an $O(a^2)$-improved gauge action [6]. Furthermore, they computed the coefficients of the operators in the action through one-loop order in lattice perturbation theory [7]. This improvement condition does not provide a unique action. The choice which is the most efficient in terms of computational effort adds a 1×2 rectangle and a 6-link "twisted" loop to the Wilson plaquette action. (See Fig. 1.)

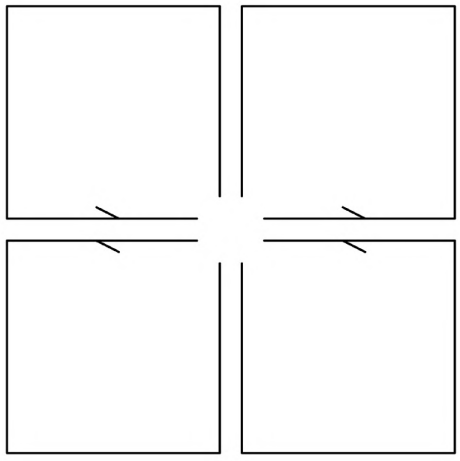

FIG. 2. The clover term in the Sheikholeslami-Wohlert action.

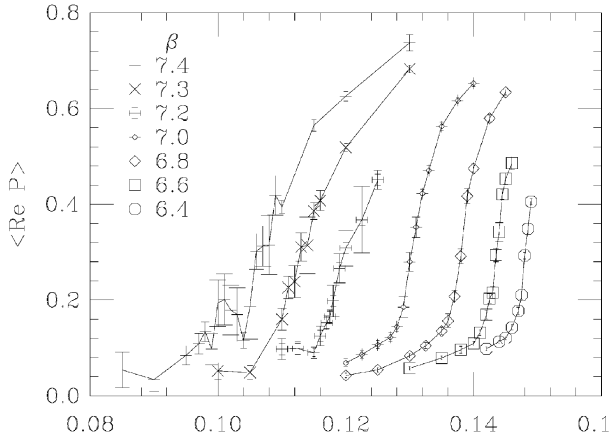

FIG. 3. Polyakov loop vs hopping parameter—all β's.

It is well known now that lattice perturbation theory in the bare coupling g_0 is not trustworthy. The a^2 in the vertex of the tadpole graph is canceled by the ultraviolet divergence of the gluon loop. Therefore, hidden in the higher order terms of the expansion in a are tadpole graphs which give an effective $a^0\Sigma_n c_n g^{2n}$ contribution. A standard way to deal with this problem is to define a mean link u_0 and replace $U_\mu \to U_\mu/u_0$ [8,9]. This introduces a "boosted" coupling constant $g^2 = g_0^2/u_0^4$.

Here we combine these two ideas, Symanzik improvement of the action and "tadpole improvement" of lattice perturbation theory. Our gauge action for this work is as derived in Ref. [10],

$$S_g = \beta \sum_{\text{plaq}} \frac{1}{3}\,\text{ReTr}(1 - U_{\text{plaq}}) + \beta_1 \sum_{\text{rect}} \frac{1}{3}\,\text{ReTr}(1 - U_{\text{rect}}) + \beta_2 \sum_{\text{twist}} \frac{1}{3}\,\text{ReTr}(1 - U_{\text{twist}}), \quad (1)$$

where β is a free parameter (in this normalization $\beta = (6/g^2u_0^4)5/3[1 - 0.1020g^2 + O(g^4)]$), and

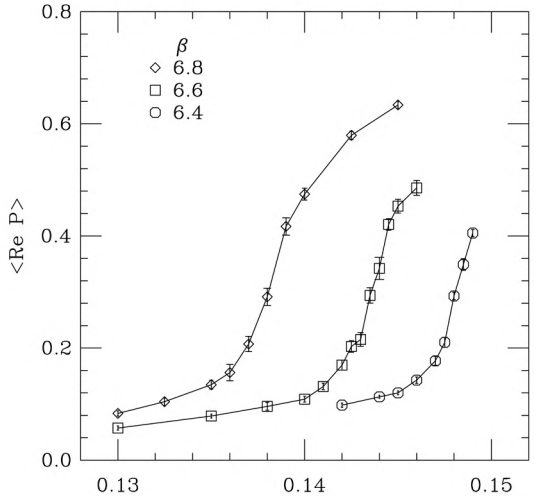

FIG. 4. Polyakov loop vs hopping parameter for the three lowest β's.

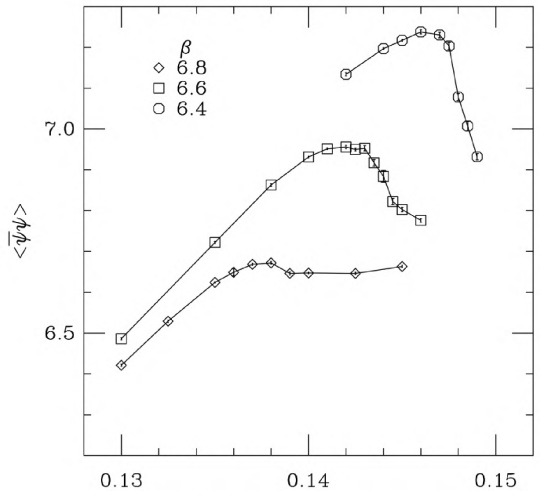

FIG. 5. $\langle\bar{\psi}\psi\rangle$ vs hopping parameter.

$$\beta_1 = -\frac{\beta}{20u_0^2}\left[1+0.4805\left(\frac{g^2}{4\pi}\right)\right] = -\frac{\beta}{20u_0^2}[1-0.6264\ \ln(u_0)], \tag{2}$$

$$\beta_2 = -\frac{\beta}{u_0^2}\,0.03325\left(\frac{g^2}{4\pi}\right) = \frac{\beta}{u_0^2}\,0.04335\ \ln(u_0). \tag{3}$$

The subscripts ''plaq,'' ''rect,'' and ''twist'' refer to the 1×1 plaquette, the planar 1×2 rectangle, and the ''$x,y,z,-x,-y,-z$'' loop, respectively. Following Ref. [9] we have chosen to define the mean link u_0 through

$$u_0 \equiv \left(\frac{1}{3}\,\mathrm{ReTr}\langle U_{\mathrm{plaq}}\rangle\right)^{1/4}, \tag{4}$$

and the strong coupling constant is defined through the perturbative expansion of the plaquette [11],

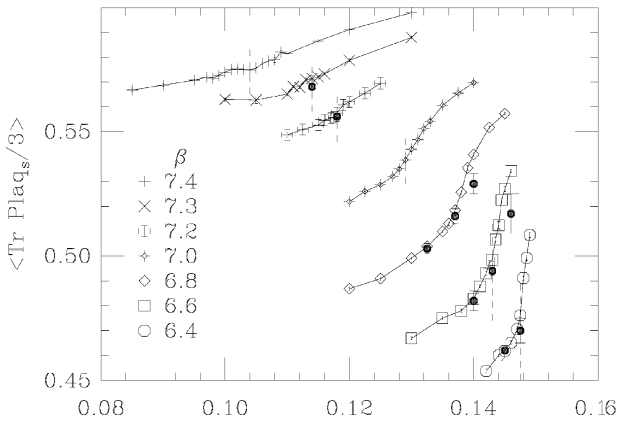

FIG. 6. Space-space plaquette vs hopping parameter—all β's. The shaded octagons mark the zero temperature values.

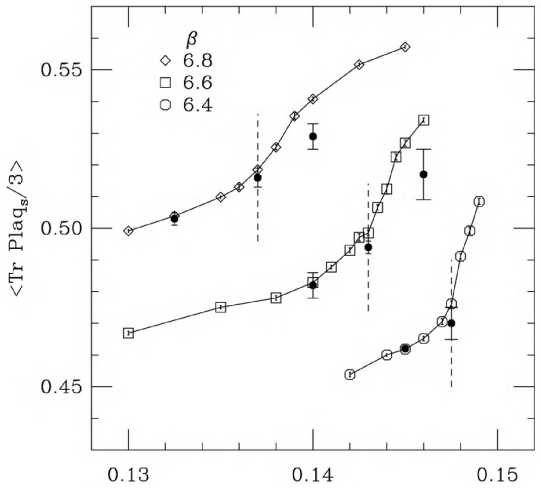

FIG. 7. Space-space plaquette vs hopping parameter for the three lowest β's. The shaded octagons mark the zero temperature values. The dashed lines indicate our determination of $\kappa_T(\beta)$ and emphasize the agreement between the spacelike plaquettes measured on zero temperature and finite temperature lattices at the crossover.

$$\frac{g^2}{4\pi} \equiv -\frac{\ln\left(\frac{1}{3}\,\mathrm{ReTr}\langle U_{\mathrm{plaq}}\rangle\right)}{3.06839}. \tag{5}$$

In the Monte Carlo simulations, we tune u_0 in the action to be consistent with the fourth root of the average plaquette. This procedure is discussed in more depth in Sec. III.

The Wilson fermion action has errors of $O(a)$. The Symanzik-improvement program can be extended to improving this action too. In the $a\to0$ limit, the $O(a)$ term in the action is proportional to $\bar{\psi}D^2\psi$ and can be removed by adding a next-nearest-neighbor operator to the action [12] or, after an isospectral transformation of the fermion fields, by adding a magnetic interaction [13]. Thus, the tree-level Symanzik-improved action is

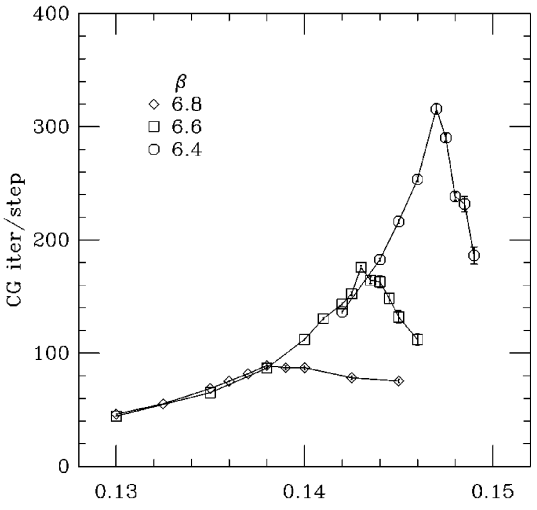

FIG. 8. Conjugate gradient matrix inversions vs hopping parameter.

TABLE I. Best fits to the masses of the pseudoscalar and vector mesons on an $8^3\times16$ lattice. Points marked by an asterisk lie on the $N_t=4$ crossover. The No. column lists the number of propagators used to compute spectroscopy.

β	κ	u_0	No.	$aM_{\rm PS}$	$t_{\rm range}$	$aM_{\rm V}$	$t_{\rm range}$	$M_{\rm PS}/M_{\rm V}$
*6.40	0.145	0.826	81	0.931(4)	2–5	1.351(18)	4–7	0.689(10)
*6.40	0.1475	0.828	30	0.664(8)	4–8	1.26(6)	4–7	0.527(26)
6.60	0.140	0.834	64	1.173(4)	5–8	1.481(9)	4–7	0.792(6)
*6.60	0.143	0.841	144	0.927(4)	4–7	1.280(8)	3–8	0.724(6)
6.60	0.146	0.855	40	0.468(15)	3–6	1.04(13)	4–7	0.45(6)
6.80	0.1325	0.842	79	1.494(3)	6–8	1.700(7)	6–8	0.879(4)
*6.80	0.137	0.849	120	1.187(3)	4–7	1.421(6)	4–8	0.835(4)
6.80	0.140	0.857	43	0.885(8)	3–6	1.182(16)	4–7	0.749(12)
*7.20	0.118	0.864	143	1.915(3)	4–8	1.994(3)	4–8	0.960(2)
*7.30	0.114	0.8695	30	2.043(4)	3–8	2.106(5)	2–8	0.970(3)

$$S_f = S_W - \frac{\kappa}{u_0^3}\sum_x \sum_{\mu<\nu} [\bar{\psi}(x) i\sigma_{\mu\nu}F_{\mu\nu}\psi(x)], \qquad (6)$$

where S_W is the usual Wilson fermion action, and

$$iF_{\mu\nu} = \frac{1}{8}(f_{\mu\nu} - f_{\mu\nu}^\dagger). \qquad (7)$$

$f_{\mu\nu}$ is the clover-shaped combination of links (see Fig. 2). As with the gauge action, the links here are also tadpole improved. Note that one factor of u_0 is absorbed into the hopping parameter.

Both these gauge and fermion actions have been used widely, e.g., in studies of finite temperature SU(3) [14,15] and quenched spectroscopy [16–18]. At least one group is in the process of using this action to calculate spectroscopy on unquenched configurations [19]. Therefore, we believe our choice of action to be well justified and useful for comparison to other work.

Of course, further progress is being made in refining the Symanzik-improvement program. One can attempt to set the coefficients of the higher dimension operators nonperturbatively by demanding that, for example, Ward identities be satisfied up to some order in the lattice spacing [20]. Also, fermion actions which are constructed to have errors of $O(a^3)-O(a^4)$ are currently being tested [21,22].

III. SIMULATION DETAILS

Our finite temperature simulations were on an $8^3\times4$ lattice. At fixed β (=6.4, 6.6, 6.8, 7.0, 7.2, 7.3, and 7.4) we varied κ in small increments across the crossover. For the updating, we used the standard hybrid molecular dynamics (HMD) algorithm [23] followed by a Monte Carlo accept or reject step [hybrid Monte Carlo (HMC) algorithm] [24]. The calculation of the ''clover'' contribution to the HMD equations of motion is tedious but straightforward.[1] The even-odd preconditioning technique developed for standard Wilson fermions [26] is also implemented for the improved Wilson fermion action [27]. Our microcanonical time step was such that the acceptance rate was between 60% and 80%; typically $\Delta t=0.03$, but for the stronger gauge coupling (lighter quark mass) runs $\Delta t=0.01$. We accumulated over 1000 trajectories at points close to the crossover.

Our companion zero temperature runs were performed on an $8^3\times16$ lattice at five (β,κ) points along the crossover, as well as at five other points neighboring the crossover line. Some of these runs were extended in order to be able to extract the heavy quark potential from Wilson loop expectation values. As with the finite temperature runs, we tried to maintain a Monte Carlo acceptance rate around 60–80%, and so our time step varied from $\Delta t=0.005$ to 0.03. Measurements of hadron correlators and Wilson loops were taken every ten trajectories.

The large majority of our simulations were performed on the IBM SP2 at the Cornell Theory Center, and two finite temperature simulations were run on a cluster of IBM RS/6000's at the Supercomputer Computations Research Institute of Florida State University.

We used the conjugate gradient (CG) matrix inversion algorithm to compute $(M^\dagger M)^{-1}$ with a maximum residue of 10^{-6} during the HMC updating. For the spectroscopy calculations, where we wish to invert M, we found the stabilized biconjugate gradient (biCGstab) algorithm to be twice as efficient as CG [28].

We tuned u_0 so that it agreed with the fourth root of the spacelike plaquettes that we measured. It might have been

TABLE II. Best fits to the mass of the nucleon.

β	κ	u_0	No.	aM_N	$t_{\rm range}$	$M_N/M_{\rm V}$
6.40	0.145	0.826	81	2.14(3)	4–7	1.58(3)
*6.40	0.1475	0.828	30	1.63(11)	4–8	1.29(11)
6.60	0.140	0.834	64	2.30(3)	5–8	1.55(2)
*6.60	0.143	0.841	144	1.958(18)	3–6	1.530(15)
6.60	0.146	0.855	40	1.34(5)	2–5	1.29(17)
6.80	0.1325	0.842	79	2.651(13)	6–8	1.56(1)
*6.80	0.137	0.849	120	2.190(10)	3–6	1.541(10)
6.80	0.140	0.857	43	1.75(4)	2–8	1.48(4)
*7.20	0.118	0.864	143	3.110(5)	4–8	1.560(3)
*7.30	0.114	0.8695	30	3.297(11)	2–7	1.614(6)

[1]Independent of our work, calculations of the HMD equations of motion for this improved Wilson fermion action have been published in [25].

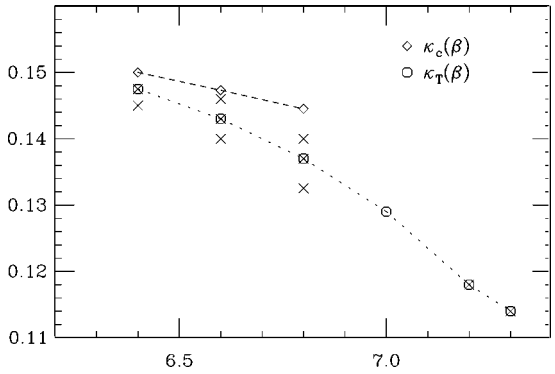

FIG. 9. Phase diagram for the Symanzik-improved action. Octagons represent the $N_t=4$ thermal crossover, and diamonds indicate estimates of the locations of vanishing pion mass. Zero temperature simulations were performed at the crosses. Dashed and dotted lines are merely to guide the eye.

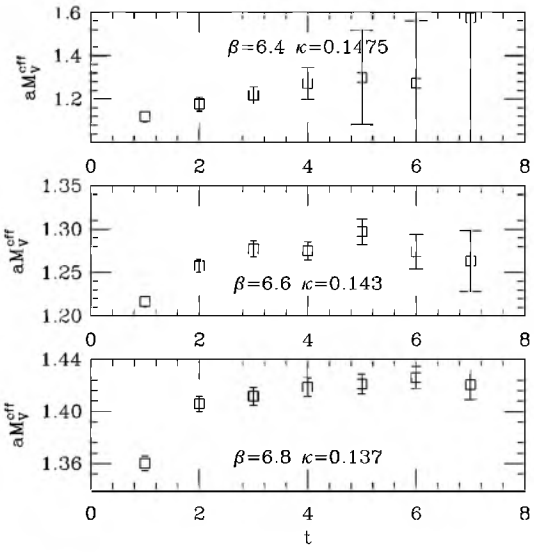

FIG. 10. Effective vector meson mass plots along the thermal crossover for $\beta=6.4,6.6,6.8$.

preferable to do this on $T=0$ configurations; however, the heavy cost of repeatedly equilibrating an $N_t=16$ lattice forced us to perform this tuning procedure on the $N_t=4$ configurations. In the next section we will show that the difference in the two ways of tuning u_0 is small. This tuning procedure would be dangerous if the system underwent a first order phase transition, but we will also show that the plaquette varies smoothly across the transition. Let us remark that this tuning procedure is a prescription. u_0 may be defined in a number of ways since it is an *estimate* of the higher order tadpole contributions to perturbation theory calculations. Therefore, while one might argue that tuning u_0 strictly on a zero temperature lattice would better estimate the tadpole contributions, our method is well defined and self-consistent.

IV. RESULTS

A. Thermodynamics

The first task was to locate the thermal crossover line $\kappa_T(\beta)$. To this end we measured the expectation values of the Polyakov loop, the plaquette, the quark condensate $\langle\bar{\psi}\psi\rangle$, and the number of CG matrix inversion iterations as we generated the $8^3\times4$ configurations.

In pure gauge theory the Polyakov loop is an order parameter for the deconfinement transition: $\langle P\rangle=0$ in the confined phase because the free energy for a single color triplet charge is infinite, while in the deconfined phase the test charge can be screened; so the free energy is finite and $\langle P\rangle \neq 0$. For unquenched QCD, the Polyakov loop is not an order parameter since it is nonzero even in the hadronic phase, but it does increase dramatically at the transition. In this work, we identify the thermal crossover as the place where the derivative of $\langle \mathrm{Re}P\rangle$ is greatest. Figure 3 shows $\langle \mathrm{Re}P\rangle$ versus the hopping parameter κ for the seven values of fixed coupling β. Figure 4 shows only the runs where the crossover is at the lowest three values of $M_{\mathrm{PS}}/M_{\mathrm{V}}$. Although the crossover becomes steeper at stronger coupling, there is no evidence of a first order transition.

In continuum QCD with massless quarks, one expects to see a restoration of the spontaneously broken chiral symmetry at high temperatures. The order parameter for this transition is the chiral condensate $\langle\bar{\psi}\psi\rangle$. Since Wilson fermions break chiral symmetry explicitly, the meaning of $\langle\bar{\psi}\psi\rangle$ at $\kappa \neq \kappa_c$ is not so clear. Besides the usual multiplicative renor-

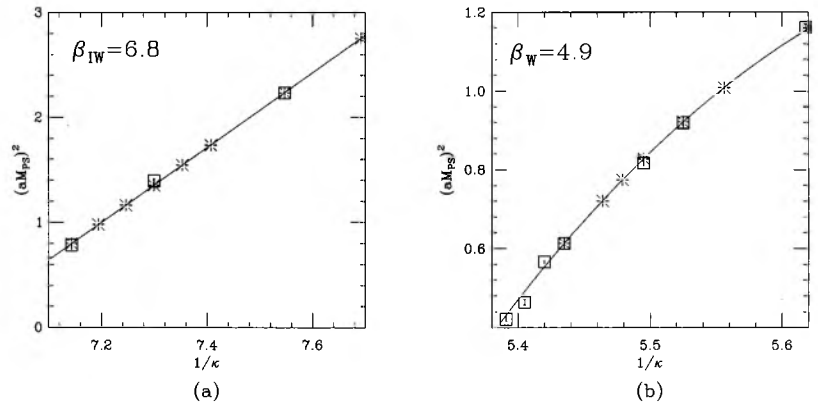

FIG. 11. Interpolation of the pseudoscalar mass squared as a function of $1/\kappa$ for (a) the improved action ($\beta_{IW}=6.8$) and (b) the unimproved action ($\beta_W=4.9$). Squares denote computed masses and asterisks mark interpolated masses.

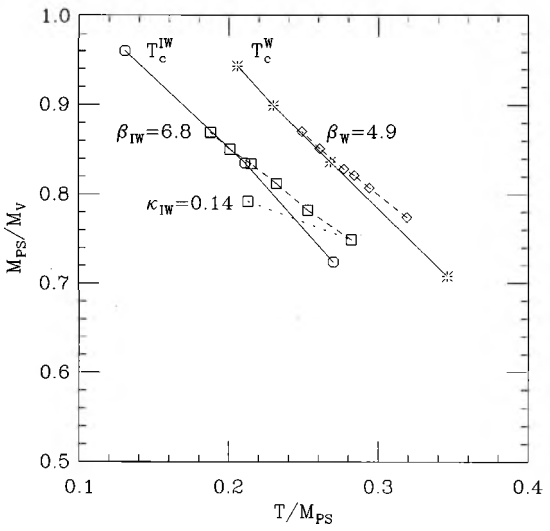

FIG. 12. The physical phase diagram. Octagons (asterisks) mark the locations of the $N_t=4$ thermal crossover for the improved (unimproved) action; solid lines connect these points. Squares (diamonds) mark points along thermodynamic simulations. Dashed lines connect points of constant β and the dotted line connects points of constant κ.

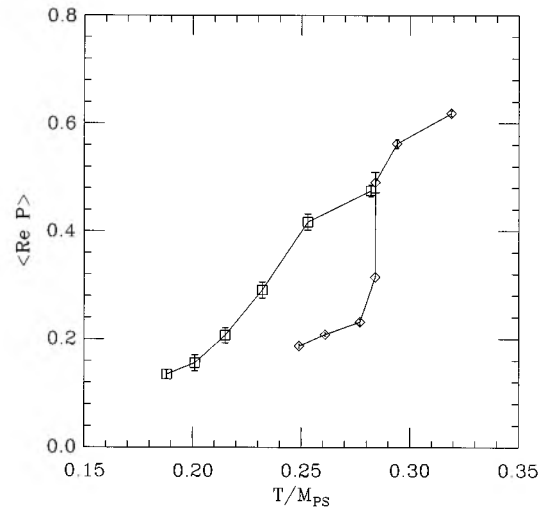

FIG. 13. Polyakov loop as a function of T/M_{PS} for fixed β. Squares: $\beta_{IW}=6.8$ improved Wilson fermions. Diamonds: $\beta_W=4.9$ unimproved Wilson fermions. Both have similar M_{PS}/M_V at the crossover.

malization one must make a subtraction to compensate for the additive renormalization of the quark mass. A properly subtracted $\langle\bar{\Psi}\Psi\rangle$ can be defined through an axial vector Ward identity [29]. However, since our study did not include calculation of screening propagators, we can only look at the unrenormalized $\langle\bar{\psi}\psi\rangle$. In spite of these problems, Fig. 5 shows a drop in $\langle\bar{\psi}\psi\rangle$ at the crossover identified by $\langle \mathrm{Re}P\rangle$.

Since we use the plaquette (in the space-space planes) to self-consistently tune u_0, we must ensure that it varies smoothly across the thermal crossover. Figures 6 and 7 show that this is the case. In fact, the plaquette on the zero temperature lattices agrees within errors with the plaquette at finite temperatures on the confined side of the crossover. The dashed vertical lines in those figures simply mark the location of the crossover $\kappa_T(\beta)$. The large errors on the deconfined side are due to the smaller sample sizes where running at lower quark mass is expensive.

As the thermal crossover line $\kappa_T(\beta)$ approaches the critical line $\kappa_c(\beta)$, the number of iterations needed to invert the fermion matrix per time step, N_{iter}, peaks at the thermal crossover. The reason is that as one approaches $\kappa_T(\beta)$ from the confined side (varying κ with β fixed) the zero modes at $\kappa_c(\beta)$ become more influential, while there are no zero modes in the deconfined phase. Figure 8 shows the peaks in N_{iter} are at the same locations as the crossovers indicated by the Polyakov loop.

B. Spectrum

For a number of reasons, it is useful to evaluate some zero temperature quantities at the parameters of our thermodynamic simulations. The light hadron spectrum is essential in determining the chiral limit for Wilson-like fermions.

The spectroscopy was an entirely straightforward lattice computation which used Gaussian-smeared source wave functions and pointlike sink wave functions. We performed correlated fits to a single exponential and selected the best fits based on a combination of smallest χ^2 per degree of

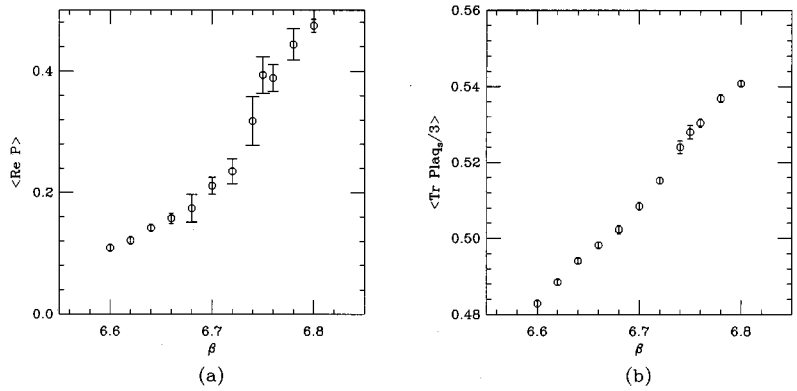

FIG. 14. Polyakov loop (a) and space-space plaquette (b) as functions of β for $\kappa=0.140$.

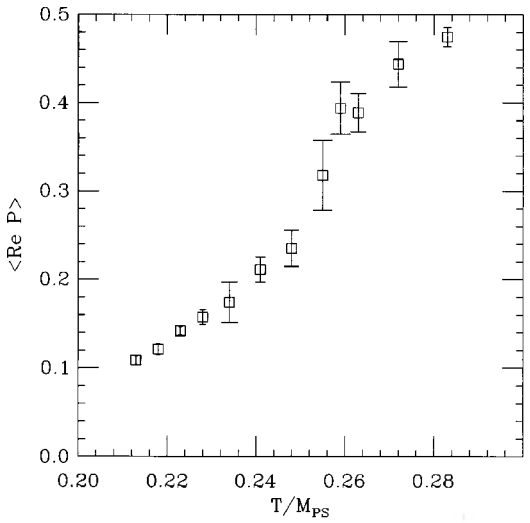

FIG. 15. Polyakov loop as a function of $T/M_{\rm PS}$ for fixed $\kappa_{IW}=0.140$.

freedom and largest confidence level. Propagators are separated by ten HMC trajectories.

Our calculations of the hadron spectrum for our zero temperature simulations are summarized in Tables I and II. The phase diagram (Fig. 9) illustrates the location of the $T=0$ runs with respect to the thermal crossover and critical lines, $\kappa_T(\beta)$ and $\kappa_c(\beta)$, respectively. An anomaly in Table I is the small data set for $\beta=6.4$, $\kappa=0.1475$. Naturally we would prefer to have more configurations with which to compute hadron correlators. Unfortunately the cost of running at those parameters is high.

One diagnostic tool for evaluating the quality of spectroscopic lattice data is an effective mass plot. One simply "fits" the hadron propagator between two successive time slices t and $t+1$ to a single exponential. (It is not really a fit because there are only two points.) When a propagator is "asymptotic" and couples only to the lightest state in that channel, one expects to see a plateau in the effective mass as t is varied. For example, we show effective mass plots for the vector meson at several points along the thermal crossover in Fig. 10.

Finite size effects could be a source of error in our calculations. If we expect our lattice spacing to be 0.25 fm or greater (this assumes $T_c \leqslant 200$ MeV), then the spatial size of our lattice is at least 2 fm. For an estimate of the finite volume errors, let us look at quenched studies with valence Wilson quarks at $\beta=5.7$, which is the critical coupling for $N_t=4$. At a quark mass corresponding to $M_{\rm PS}/M_{\rm V}=0.69$, there is a 3.3% finite size effect in the vector meson mass [30,31]. While some of our computations are at smaller quark mass, even $M_{\rm PS}/M_{\rm V}\approx 0.5$, we expect a smaller T_c, say, 150 MeV vs the 260 MeV in quenched simulations—our box size may be as large as 2.7 fm. While finite size effects are more severe in unquenched QCD than quenched QCD for box sizes less than 1.5 fm, they are comparable for larger boxes [32]. The quenched results lead us to believe that this is large enough to keep the finite volume errors under control. Therefore, we believe that finite size effects are at most a few percent, which is comparable to our statistical errors. Of course a thorough investigation of these effects is warranted if this action is to be used in a full-scale spectrum calculation.

While in Fig. 3 we do not see the same first-order jump in $\langle {\rm Re}P\rangle$ that we did with the standard Wilson actions, we would like to make the comparison more convincing. After all, we cannot know *a priori* the relation between the bare parameters for the standard action (β_W,κ_W) and those for the improved action (β_{IW},κ_{IW}); it could happen that a small change in κ_W corresponds to a much larger change in the quark mass than does a similar change in κ_{IW}, giving us the illusion that the crossover is broader for the improved action.

In continuum QCD, the quark mass m_q and the temperature T are the two parameters of the theory. Dimensionless quantities are more accessible from lattice simulations, and so we use the pseudoscalar/vector mass ratio $M_{\rm PS}/M_{\rm V}$ to represent the quark mass. The temperature can be divided by any mass scale. Ideally, we would use something which has little dependence on the quark mass, e.g., the square root of the string tension. However, the calculations of the heavy quark potential have not been performed for the standard Wilson action in this region of parameter space. Therefore, we content ourselves with using a meson mass. Let us choose the pseudoscalar for the present discussion.

First let us compare the thermal crossovers at the same value of $M_{\rm PS}/M_{\rm V}$. Data from Ref. [33] suggest that we compare $\beta_W=4.94$ and $\kappa_W=0.18$, where $M_{\rm PS}/M_{\rm V}=0.836(5)$, to our $\beta_{IW}=6.80$ and $\kappa_{IW}=0.137$, where $M_{\rm PS}/M_{\rm V}=0.835(4)$. The data we use for comparison with ours are the unimproved $\beta_W=4.9$ data provided in Refs. [1,34]. Spectroscopy was not performed at each thermodynamic data point, and so some interpolation of masses as functions of $1/\kappa$ is necessary. We interpolated the lattice pseudoscalar meson mass squared using a linear least squares fit to a quadratic in $1/\kappa$ around the crossover region for the unimproved Wilson data. As a result of the smaller data sample, we interpolated $(aM_{\rm PS})^2$ linearly in $1/\kappa$ for our improved Wilson data. Figure 11 shows these interpolations. The lattice vector meson masses were obtained similarly, interpolating $aM_{\rm V}$ rather than $(aM_{\rm V})^2$. In practice, these interpolations are not to sensitive to our fitting function, and

TABLE III. Fits to the heavy quark potential along the $N_t=4$ crossover ($n_f=2$ improved Wilson fermions).

β	κ	No.	$r_{\rm min}$-$r_{\rm max}$	t	aV_0	$a^2\sigma$	e	f	r_0/a
6.40	0.1475	30	1.41-4.47	2	1.0(3)	0.41(8)	0.7(2)	5.6(6)	1.52(4)
6.60	0.1430	108	1.41-6.93	2	0.65(9)	0.42(3)	0.34(8)	3.21(24)	1.77(2)
6.80	0.1370	95	1.41-6.93	2	0.70(6)	0.346(15)	0.38(5)	2.45(18)	1.913(13)
7.20	0.1180	117	1.41-5.66	2	0.65(2)	0.253(6)	0.33(2)	1.06(8)	2.287(13)

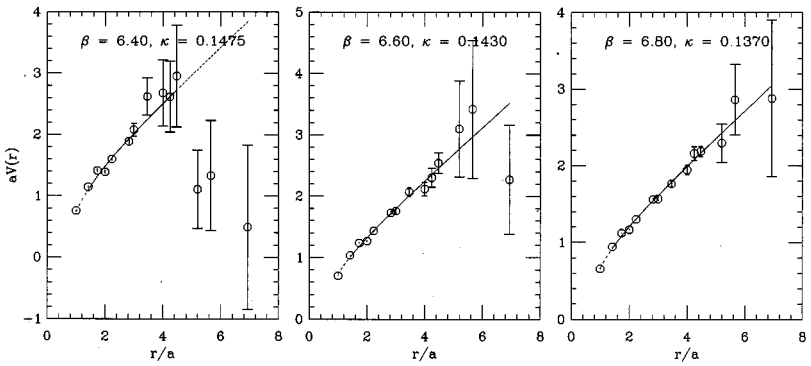

FIG. 16. The heavy quark potential from Wilson loops. Octagons are the effective potentials $V_t(\vec{r})$ and the line is the fit to the ansatz.

we are only aiming for a sound qualitative comparison of the crossover.

In Fig. 12 we show the physical phase diagram $M_{\rm PS}/M_{\rm V}$ vs $T/M_{\rm PS}$ $[T=(4a)^{-1}]$. The solid lines show the locations of the thermal crossover for the two actions. The fact that they are at different places is a direct consequence of lattice artifacts: The simulations give different physics at the same $M_{\rm PS}/M_{\rm V}$. Plotted in this figure as dashed lines are two runs at fixed β. For both runs $M_{\rm PS}/M_{\rm V}$ decreases from ≈ 0.87 to ≈ 0.78, and $T/M_{\rm PS}$ increases about 15%. The fixed β runs seem to cross the thermal crossover line at the same angle. (One must remember there is some uncertainty due to interpolation in Fig. 12 which is to be interpreted qualitatively.) When we compare the Polyakov loop along these two fixed β runs, which we argue cross $T_c/M_{\rm PS}$ similarly, we find the crossover is indeed smoother for the improved action (see Fig. 13).[2]

One might worry that the fixed β runs cross $T_c/M_{\rm PS}$ too slowly: The runs appear nearly tangential to the crossover. Perhaps if one crossed the critical line at a less acute angle the transition would be much steeper. This does not turn out to be the case. We performed an exploratory run at fixed $\kappa_{IW}=0.140$, varying β_{IW} from 6.6 to 6.8. The raw data appear in Fig. 14. This run is represented by a dotted line in Fig. 12 and crosses the critical line at a sharper angle. We only have two zero temperature runs at $\kappa=0.140$, and so our linear extrapolation of $(aM_{\rm PS})^2$ in $1/\kappa$ is not even a fit, but it is clear that the transition is smooth (see Fig. 15). On the contrary, Fig. 3 in Ref. [1] shows a stiff transition for fixed κ runs from $\kappa_W=0.12$ to $\kappa_W=0.20$.

Let us summarize this lengthy discussion. We set out to answer the question, is the transition in fact smoother for the improved action than for the unimproved action? In order to make a sound comparison between results from different actions, we needed to present our results using physical parameters. Since we have performed just a few zero temperature simulations, some interpolation was necessary in order to present thermodynamic data along specific curves in the physical phase space. Although this interpolation introduces some systematic error, the qualitative features of Figs. 12–15 are preserved barring some unlikely large deviation in Fig. 11. We would like to be able to look at the crossover at constant $M_{\rm PS}/M_{\rm V}$ or at constant T, but our simulations are limited to fixed β or κ. Therefore, we attempted to show that the qualitative shape of the Polyakov loop as one crosses the critical line is not strongly sensitive to the specific path in phase space. Since the crossover is smooth for all fixed β_{IW} and the one fixed κ_{IW} runs, and since the crossover is steep for both fixed β_W runs and fixed κ_W runs, we conclude that the transition is smoother for the improved action. The artificial first-order behavior is not present with the improved action.

Finally, we remark that, when one replaces $T/M_{\rm PS}$ by $T/M_{\rm V}$, Figs. 11–15 are qualitatively the same and our conclusions are unchanged.

C. Heavy quark potential

In addition to computing hadronic masses, we used Wilson loop data to measure the heavy (or static) quark potential $V(\vec{r})$:

$$V(\vec{r})=-\lim_{t\to\infty}\frac{1}{t}\ln W(\vec{r},t). \tag{8}$$

A standard ansatz for the form of the potential is

$$V(r)=V_0+\sigma r-\frac{e}{r}-f\left(G_L(r)-\frac{1}{r}\right), \tag{9}$$

where V_0, σ, e, and f are fit parameters, and G_L is the lattice Coulomb potential. In practice, this fit is performed for a fixed t; that is, the potential is estimated through an effective potential,

$$V_t(\vec{r})=-\ln\left[\frac{W(\vec{r},t+1)}{W(\vec{r},t)}\right], \tag{10}$$

such that

$$W(r,t)\sim\exp[-V_t(r)t]. \tag{11}$$

The parameter r_0 is defined to be the length such that

[2]Previously, this result was presented as a function of $(aM_{\rm PS})^2=(M_{\rm PS}/4T)^2$ (e.g., in Ref. [35]).

TABLE IV. Fits to the heavy quark potential along the $N_t=4(*6)$ crossovers ($n_f=2$ Kogut-Susskind fermions).

β	am_q	No.	$r_{\min}$-$r_{\max}$	t	aV_0	$a^2\sigma$	e	f	r_0/a
5.2875	0.025	55	1.41-6.93	2	0.80(10)	0.30(3)	0.46(10)	1.46(20)	1.99(4)
5.3200	0.050	67	2.24-6.93	2	0.68(22)	0.29(4)	0.2(3)	5.7(1.1)	2.17(11)
5.3750	0.100	90	1.00-5.66	3	0.62(8)	0.288(23)	0.26(7)	0.56(12)	2.20(4)
*5.415	0.0125	280	2.24-6.71	3	0.76(2)	0.130(5)	0.36(2)	1.0(2)	3.14(5)

$$r_0^2 F(r_0)=1.65, \tag{12}$$

with

$$F(r)=\frac{\partial V}{\partial r}, \tag{13}$$

which corresponds to $r_0=0.49$ fm from potential models. Sommer showed this to be a useful quantity with which to set the lattice scale [36]. In this work we calculated the force by taking numerical differences of the potential. Our analysis proceeds as in Ref. [37]. Errors are estimated by bootstrapping the data, and occasionally increased to account for differences in the choice of t. We present our fits to the potential for the zero temperature simulations along the $N_t=4$ crossover with improved Wilson fermions in Table III. Graphs of three of these fits appear in Fig. 16.

For comparison, we performed the same calculation with two flavors of Kogut-Susskind fermions for three parameter sets along the $N_t=4$ crossover. Our fits are given in Table IV. Meson masses were taken from Table 1 of Ref. [38]. In addition, we measured the potential at one point along the $N_t=6$ KS crossover. That fit also appears in Table IV. The generation and spectroscopy of those configurations are discussed in Ref. [39].

D. Scaling tests

In Secs. IV A and IV B we showed that thermodynamics with the improved action does not have the same artificial first-order behavior that unimproved Wilson thermodynamics does. However, in order to make physical predictions which can be compared with results from Kogut-Susskind thermodynamics, we must make use of the spectrum and potential computations described in the preceding two sections.

In Fig. 17 we plot the ratio T_c/M_V as a function of the pseudoscalar/vector meson mass ratio M_{PS}/M_V. Extrapolation to the physical π/ρ mass ratio is necessary in order to make a prediction for T_c. The fact that T_c/M_V is independent of N_t for the Kogut-Susskind action leads one to believe that this quantity is scaling at lattice spacing $a=1/(4T_c)$. Clearly, this statement is not true for the unimproved Wilson action. The $N_t=4$ unimproved Wilson points show a large dependence on the quark mass, and disagree significantly with the corresponding $N_t=6$ points at $M_{PS}/M_V<0.8$. In addition, since T_c/M_V is consistently lower for the improved action than the unimproved action at equal lattice spacing, the discretization errors in the latter must be appreciable. The improved Wilson point at $M_{PS}/M_V=0.53$ appears to have some slight agreement with the Kogut-Susskind data, but with a large error. Finally, we remark that one expects $T_c/M_V\to 0$ in the infinite quark mass limit since the vector meson mass diverges there, and so ultimately we want to simulate at as small M_{PS}/M_V as possible in order to extrapolate to $M_\pi/M_\rho=0.18$ reliably.

In order to look at T_c scaled by quantities which are nominally independent of the quark mass, we use $\sqrt{\sigma}$ and r_0 from our potential fits mentioned in Sec. IV C. In Fig. 18 the rise in $T_c/\sqrt{\sigma}$ and r_0T_c as $M_{PS}/M_V\to 1$ is presumably due to T_c approaching the pure SU(3) transition temperature as the quarks decouple. The $N_t=4$ quenched $T_c/\sqrt{\sigma}$ from Ref. [40] appears as an arrow in Fig. 18 and supports this presumption. The disagreement between the Kogut-Susskind and improved Wilson actions is more apparent in Fig. 18 than in Fig. 17. The error in $\sqrt{\sigma}$ is large, but both $T_c/\sqrt{\sigma}$ and r_0T_c are lower for our improved action than for the KS action. In fact, the small error in r_0 reveals the presence of quark mass dependences even at $M_{PS}/M_V=0.53$.

The quark mass effect can be identified further in the plot of $T_c/\sqrt{\sigma}$ vs $a\sqrt{\sigma}$ (Fig. 19). Since $a=1/(4T_c)$ for all of the $N_t=4$ data, the spread in $a\sqrt{\sigma}$ for the improved action is caused by the increase in the deconfinement temperature as the quarks become infinitely heavy. One should contrast to this the observation that the three $N_t=4$ KS points lie on top of each other. The higher N_t points for both KS and

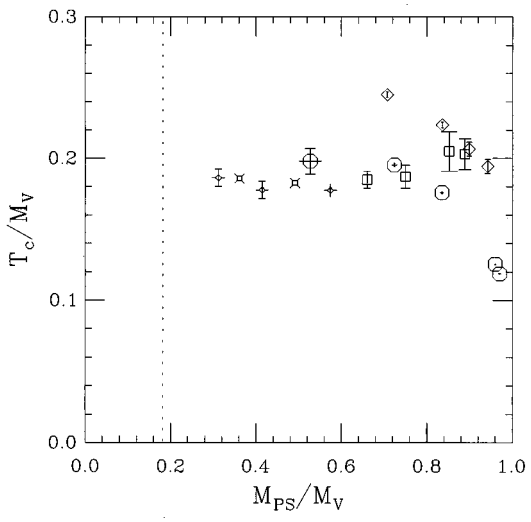

FIG. 17. Critical temperature divided by vector meson mass vs pseudoscalar/vector meson mass ratio. Our data for $N_t=4$ improved Wilson actions are the octagons. Diamonds: $N_t=4$ unimproved Wilson. Square: $N_t=6$ unimproved Wilson. Fancy diamonds and squares: $N_t=4,6$ Kogut-Susskind (KS), respectively [2].

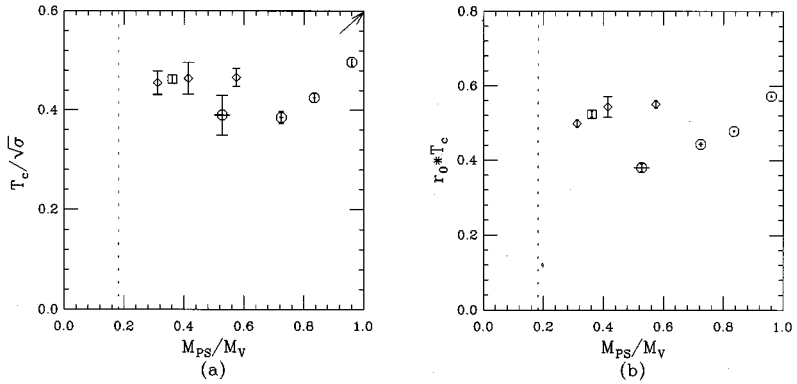

FIG. 18. Critical temperature scaled by (a) the square root of the string tension and (b) the inverse Sommer parameter vs pseudoscalar/vector meson mass ratio. Octagons: $N_t=4$ improved Wilson. Diamonds: $N_t=4$ KS. Square: $N_t=6$ KS. The arrow in (a) shows the $N_t=4$ quenched $T_c/\sqrt{\sigma}$ from Ref. [40].

quenched actions show their relative independence on lattice spacing. The conclusion one should draw from Figs. 18 and 19 is that in the case of the improved Wilson data, any attempt at extrapolation to physical quark mass is premature.

In Fig. 20 we plot $r_0\sqrt{\sigma}$ vs a/r_0. While r_0 and $\sqrt{\sigma}$ are independent of a/r_0 and m_q within the error bars, the variation in a/r_0 for the improved action along the crossover is another manifestation of the quark mass dependence of the critical temperature. A plot against $a\sqrt{\sigma}$ looks qualitatively the same, but with larger errors.

A graph of the vector meson mass times r_0 (Fig. 21) shows nice behavior for the Kogut-Susskind simulations, disagreement between KS and clover, and the rise in M_V toward infinity at large M_{PS}/M_V. Again, we do not show $M_V/\sqrt{\sigma}$ vs M_{PS}/M_V since it is qualitatively the same, but with larger error bars. If we were so bold as to argue that the improved Wilson data could be extrapolated to physical M_π/M_ρ using the points $M_{PS}/M_V \leq 0.8$, then we would conclude $M_V/\sqrt{\sigma}$ for our action is less than for the Kogut-Susskind action. This would not be too surprising given similar trends in scaling violations for quenched QCD spectroscopy as presented in Fig. 2 of Ref. [18], for example. At finite lattice spacing, $M_\rho/\sqrt{\sigma}$ computed with KS valence quarks lies above the $a=0$ extrapolation, while unimproved Wilson quark calculations give a value less than the continuum number. The addition of the clover term significantly reduces this scaling violation; however, the lattice value of $M_\rho/\sqrt{\sigma}$ still lies below its continuum value. Of course, in the absence of clear scaling between M_V and $\sqrt{\sigma}$ (and r_0), such arguments in this work are speculative.

V. CONCLUSIONS

This is the first large scale simulation of unquenched QCD with improved Wilson fermions of which we are aware. We find that the Symanzik-improvement program, at this level, fulfills its promise in that a serious lattice artifact, the spurious first-order transition at intermediate hopping parameters, has been removed. The thermal crossover does become progressively steeper as one decreases the quark mass, but it is smooth in the sense that the Polyakov loop and the

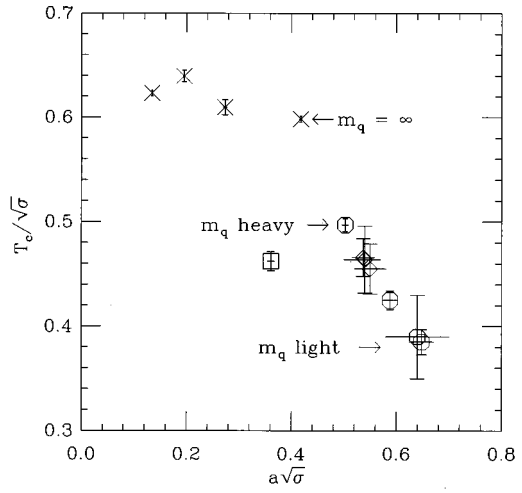

FIG. 19. Critical temperature scaled by the square root of the string tension (left) vs the lattice spacing in units of $1/\sqrt{\sigma}$. Octagons: $N_t=4$ improved Wilson. Diamonds: $N_t=4$ KS. Square: $N_t=6$ KS. Crosses: quenched SU(3) from Ref. [40].

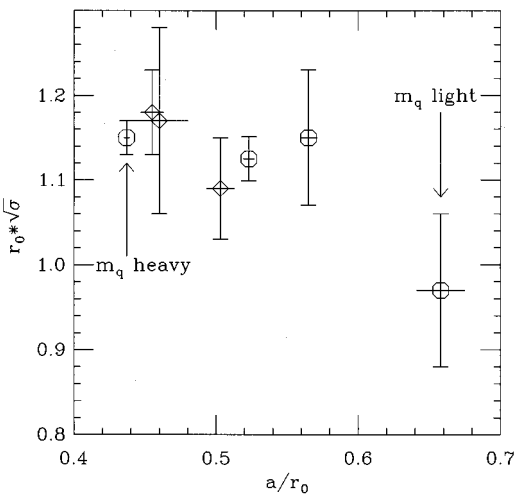

FIG. 20. The dimensionless quantity $r_0\sqrt{\sigma}$ vs the lattice spacing in units of r_0. Octagons: $N_t=4$ improved Wilson. Diamonds: $N_t=4$ KS.

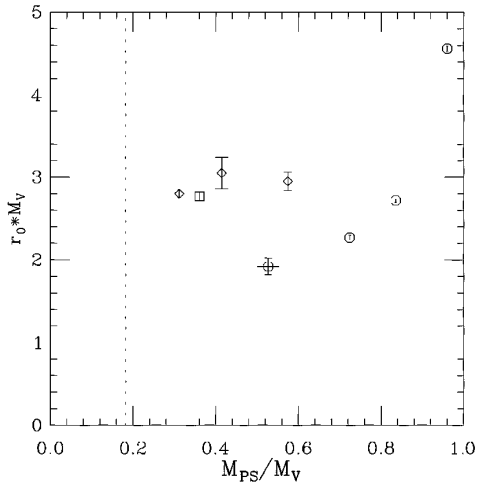

FIG. 21. Vector meson mass times r_0 vs pseudoscalar/vector meson mass ratio. Octagons: $N_t=4$ improved Wilson. Diamonds: $N_t=4$ KS. Square: $N_t=6$ KS.

plaquette are single valued for all (β,κ) at which we computed.

However, improvement at this order is no panacea. It is still very costly to invert the fermion matrix near and below $M_{\rm PS}/M_{\rm V}\approx 0.5$. Since the critical temperature and the vector meson mass show a significant dependence on the quark mass, extrapolation to M_π/M_ρ is not trustworthy. Furthermore, disagreement is evident in $T_c/\sqrt{\sigma}$ and $M_{\rm V}r_0$ between our improved Wilson action and the unimproved Kogut-Susskind formulation, even at comparable $M_{\rm PS}/M_{\rm V}$.

One cannot yet use this disagreement to cast doubt on the Kogut-Susskind results because the scaling behavior of the improved Wilson action has not been sufficiently tested. Simulations with smaller lattice spacing, perhaps $N_t=6$, would give a more concrete picture of the extent of scaling violations in this action.

Before beginning such an expensive undertaking, however, let us speculate as to the shortcomings of the present action in the context of thermodynamics. In the high temperature phase, thermodynamic quantities are dominated by high momentum contributions. Therefore, one must not only improve the effects of the finite lattice spacing, but also the dispersion relation at all momenta. Although the gauge action we used has a dispersion relation closer to the continuum than the plaquette action, the clover term does not change the fermionic dispersion relation from that of the unimproved Wilson action. The work with an improved gauge action but standard Wilson fermions by Ref. [4] shows improvement similar to ours, viz., removal of the jump discontinuity in the Polyakov loop. A detailed comparison of the critical temperature from their action versus ours and the standard Wilson and KS actions remains to be made.

Therefore, it is plausible that improvement of the gauge action is responsible for the removal of the artificial first-order behavior at intermediate values of the Wilson hopping parameter. However, improvement of the fermion action probably plays a role in the closer agreement to the KS results for $T_c/M_{\rm V}$, as was found in studies of quenched spectroscopy. Persistent quark mass dependence and apparent disagreement between our results and KS results for T_c scaled by quark potential parameters indicate that further improvement in the fermionic sector is warranted. One might consider using Wilson-type fermions with an improved dispersion relation in the next large scale thermodynamics study.

ACKNOWLEDGMENTS

This work was supported by the U.S. Department of Energy under Contracts Nos. DE-AC02-76CH-0016, DE-FG03-95ER-40894, DE-FG03-95ER-40906, DE-FG05-85ER250000, DE-FG05-96ER40979, DE-2FG02-91ER-40628, and DE-FG02-91ER-40661, and National Science Foundation Grants Nos. NSF-PHY93-09458, NSF-PHY96-01227, and NSF-PHY91-16964. Simulations were carried out at the Cornell Theory Center, the Supercomputer Computations Research Institute at Florida State University, and at the San Diego Supercomputer Center. One of us (M.W.) would like to extend thanks to A. Hasenfratz for several helpful discussions and to N. Christ, F. Karsch, and A. Ukawa for thoughtful comments. We also thank Craig McNeile and Tom Blum for critical readings of the manuscript.

[1] C. Bernard, T. DeGrand, C. DeTar, S. Gottlieb, A. Hasenfratz, L. Kärkkäinen, D. Toussaint, and R. L. Sugar, Phys. Rev. D **49**, 3574 (1994).

[2] C. Bernard, M. Ogilvie, T. DeGrand, C. DeTar, S. Gottlieb, A. Krasnitz, R. L. Sugar, and D. Toussaint, Phys. Rev. D **46**, 4741 (1992); T. Blum, T. DeGrand, C. DeTar, S. Gottlieb, A. Hasenfratz, L. Kärkkäinen, D. Toussaint, and R. L. Sugar, *ibid.* **50**, 3377 (1994).

[3] Y. Iwasaki, Nucl. Phys. **B258**, 141 (1985); Tsukuba Report No. UTHEP-118, 1983 (unpublished).

[4] Y. Iwasaki, K. Kanaya, S. Kaya, and T. Yoshié, Phys. Rev. Lett. **78**, 179 (1997).

[5] K. Symanzik, in *Recent Developments in Gauge Theories*, edited by G. 't Hooft *et al.* (Plenum, New York, 1980), p. 313; in *Mathematical Problems in Theoretical Physics*, edited by R. Schrader *et al.* (Springer, New York, 1982); Nucl. Phys. **B226**, 187 (1983); **B226**, 205 (1983).

[6] P. Weisz, Nucl. Phys. **B212**, 1 (1983); M. Lüscher and P. Weisz, Commun. Math. Phys. **97**, 59 (1985).

[7] M. Lüscher and P. Weisz, Phys. Lett. **158B**, 250 (1985).

[8] G. Parisi, in *High Energy Physics—1980*, Proceedings of the XXth International Conference, Madison, Wisconsin, edited by L. Durand and L. G. Pondrom, AIP Conf. Proc. No. 68 (AIP, New York, 1981).

[9] G. P. Lepage and P. B. Mackenzie, Phys. Rev. D **48**, 2250 (1993).

[10] M. Alford, W. Dimm, G. P. Lepage, G. Hockney, and P. B. Mackenzie, Phys. Lett. B **361**, 87 (1995).

[11] P. Weisz and R. Wohlert, Nucl. Phys. **B236**, 397 (1984).

[12] H. W. Hamber and C. M. Wu, Phys. Lett. **133B**, 351 (1983).

[13] B. Sheikholeslami and R. Wohlert, Nucl. Phys. **B259**, 572 (1985).
[14] B. Beinlich, F. Karsch, and E. Laermann, Nucl. Phys. **B462**, 415 (1996).
[15] B. Beinlich, F. Karsch, and A. Piekert, Phys. Lett. B **390**, 268 (1997).
[16] UKQCD Collaboration, R. Kenway, in *Lattice '96*, Proceedings of the International Symposium, St. Louis, Missouri, edited by C. Bernard *et al.* [Nucl. Phys. (Proc. Suppl.) **53**, 206 (1997)].
[17] S. Collins, R. G. Edwards, U. M. Heller, and J. Sloan, in *Lattice '96* [16], p. 877.
[18] S. Collins, R. G. Edwards, U. M. Heller, and J. Sloan, Proceedings of ''Multi-Scale Phenomena and Their Simulation,'' Bielefeld, Germany 1996, hep-lat/9611022.
[19] R. G. Edwards (private communication).
[20] M. Lüscher, S. Sint, R. Sommer, P. Weisz, and U. Wolff, Nucl. Phys. **B491**, 323 (1997).
[21] M. Alford, T. R. Klassen, and G. P. Lepage, Nucl. Phys. **B496**, 377 (1997).
[22] W. Wetzel, Phys. Lett. **136B**, 407 (1984); T. Eguchi and N. Kawamoto, Nucl. Phys. **B430**, 609 (1984); H. R. Fiebig and R. M. Woloshyn, Phys. Lett. B **385**, 273 (1996); R. Lewis and R. M. Woloshyn, Phys. Rev. D **56**, 1571 (1997).
[23] S. Gottlieb, W. Liu, D. Toussaint, R. L. Renken, and R. L. Sugar, Phys. Rev. D **35**, 2531 (1987).
[24] S. Duane, A. D. Kennedy, B. J. Pendleton, and D. Roweth, Phys. Lett. B **195**, 216 (1987).
[25] X-Q. Luo, Comput. Phys. Commun. **94**, 119 (1996); K. Jansen and C. Liu, *ibid.* **99**, 221 (1997).
[26] T. DeGrand and P. Rossi, Comput. Phys. Commun. **60**, 211 (1990).
[27] UKQCD Collaboration, C. R. Allton *et al.*, Nucl. Phys. **B407**, 331 (1993).
[28] For a recent review of matrix inversion algorithms in the field, see A. Frommer, in *Lattice '96* [16], p. 120.
[29] M. Bochicchio *et al.*, Nucl. Phys. **B262**, 331 (1985).
[30] F. Butler *et al.*, Phys. Rev. Lett. **70**, 2849 (1993); Nucl. Phys. **B430**, 170 (1994).
[31] S. Gottlieb, in *Lattice '96* [15], p. 155.
[32] S. Aoki *et al.*, Phys. Rev. D **50**, 486 (1994).
[33] K. M. Bitar *et al.*, Phys. Rev. D **43**, 2396 (1991).
[34] The Wilson meson masses were provided by K. M. Bitar *et al.*, Phys. Rev. D **54**, 3546 (1996); and (private communication).
[35] C. Bernard *et al.*, Nucl. Phys. B (Proc. Suppl.) **53**, 446 (1997).
[36] R. Sommer, Nucl. Phys. **B411**, 839 (1994).
[37] U. M. Heller, K. M. Bitar, R. G. Edwards, and A. D. Kennedy, Phys. Lett. B **335**, 71 (1994).
[38] T. Blum, L. Kärkkäinen, D. Toussaint, and S. Gottlieb, Phys. Rev. D **51**, 5153 (1995).
[39] C. Bernard, T. Blum, T. A. DeGrand, C. DeTar, S. Gottlieb, A. Krasnitz, R. L. Sugar, and D. Toussaint, Phys. Rev. D **48**, 4419 (1993).
[40] G. Boyd, J. Engels, F. Karsch, E. Laermann, C. Legeland, M. Lütgemeier, and B. Petersson, Phys. Rev. Lett. **75**, 4169 (1995).